

Failure Investigation of a Furnace Tube Support

A. M. Babakr · A. Al-Ahmrai · K. Al-Jumayiah ·
F. Habiby

Submitted: 4 April 2008 / in revised form: 30 October 2008 / Published online: 9 December 2008
© ASM International 2008

Abstract A furnace tube support failed after 6 months service at 850 °C. The support was an HK alloy, a member of the heat-resistant cast alloy family (H-Series) steels. The H-series steels are widely used in the petrochemical industry for components requiring enhanced high-temperature properties. Microstructural changes occurring at high temperature clearly affect the mechanical properties. The property degradation in HK-40 steel furnace tube support subjected to high temperature was caused by the formation of sigma phase. The investigation included metallurgical analysis, materials characterization, and mechanical analysis.

Keywords Sigma phase · Corrosion · Microstructure · Heat-resistant steels · Hardness

Introduction

Many components within oil, gas, thermal-power, chemical, and petrochemical plants are made from cast heat-resistant alloys “HRA” to accommodate the operating high-temperature environments. These alloys are experiencing a variety of degrading mechanisms. As the reliability sector of these plants evolve, assessment of damage and risk associated with the equipment using these alloys becomes important. Therefore, knowledge of potential mechanisms of degradation, the rate at which damage propagates in each

component, and how the damage manifests itself are fundamental in making proper assessments. The HRA drives its resistance because of the combinational effects of Fe-Ni-Cr “HP” or Fe-Cr-Ni “HK.”

The majority of the reported deterioration in high-temperature operating components are creep damage [1–5], microstructural degradation [6–8], high-temperature fatigue [9–11], creep fatigue [12–14], sigma-phase embrittlement [15–19], carburization [20–22], hydrogen damage, graphitization, thermal shock, erosion, liquid metal embrittlement, and high-temperature corrosion of various types. Generally, virtually all failures are the result of microstructural changes at high temperature. Most of microstructural changes occur to alloy carbides constituents [23, 24]. HRA such as HP and HK alloys original microstructure will consists of an austenite matrix with fine dispersions of carbides (Cr-rich $M_{23}C_6$ or Nb-rich MC, depending on the alloy) in the matrix along with clusters of NbC and $M_{23}C_6$ in the interdendritic regions and dispersions of $M_{23}C_6$ along the seams between dendrite colonies [25, 26].

Microstructural changes in these alloys will only occur at elevated temperatures. For example, at 590 to 650 °C (1100 to 1200 °F), precipitation starts at regions near interdendritic and will continue with further exposure to the same temperature range. Carbon supply and depletion from the nearby regions is the controlling factor in the precipitation process and in the growth of the carbides. As the component operating temperature increases beyond 650 to 970 °C (1200 to 1778 °F), carbides begin to coalesce, causing a decrease in the number of precipitates and a diminishing amount of the amount of noncoalesced carbides. At much higher temperatures, carbides become coarse and bulky. Theoretically, carbides coarsening at temperatures slightly below 1200 °C (2192 °F) reverses the coalescence process [15–26]. Precipitated carbides within

A. M. Babakr (✉) · A. Al-Ahmrai · K. Al-Jumayiah ·
F. Habiby
Saudi Basic Industries Corporation (SABIC),
SABIC Technology Center-Jubail, P.O. Box 11669,
Al-Jubail 31961, Saudi Arabia
e-mail: alibabakr@yahoo.com

the matrices begin to reverse back into solution. In reality, this can only partially take place, and the solution process is hindered by many operational parameters and differs with the type of alloy [27, 28]. Experimentally, $M_{23}C_6$ is predicted to be stable in HP6301 up to about 1250 °C (2282 °F) and to about 1282 °C (2340 °F) in HPCoW [28].

If the alloys remain at an operating temperature high enough to allow carbides (metal carbides) to grow, they become sensitized. A counterpart to sensitization is the formation of sigma “ σ ” phase (metal-iron/metal-metal phase). Although sigma phase has a different composition, the carbides in the formation process are somewhat similar in location and precipitation mechanisms.

The precipitation of σ -phase is detrimental to the crevice and pitting corrosion resistance of the alloy [29, 30]. Formation temperatures reported in open literature vary, but there is general agreement that sigma phase forms in the range of 620 to 900 °C (1148 to 1652 °F). The rate of formation and growth of σ -phase increases as temperature is raised to 800 °C (1472 °F) [31, 32] and has deleterious effects on the mechanical properties of the alloy. On the other hand, it has been reported [33, 34] that σ -phase will dissolve if held at 1000 °C. This investigation has correlated formation and presence of σ -phase in heat-resistant cast material HK-40 to the degradation in mechanical properties both at low and high temperatures.

Investigation and Results

HK-40 cast samples were cut from the failed furnace tube that had experienced prolonged exposure to approximately 850 °C (1562 °F). The HK-40 was used as a structural support inside a furnace. The exposure duration was no more than 6 months or 4000 h. During operation, the tree support alloy was subjected to regular operation, decoking regimes, and shutdowns, and other sudden failures occurred. Several samples suffered high-temperature cracking, and all had similar features to those found in the component investigated.

Figure 1 shows a fracture surface of one of the furnace tube supports. Clearly, the fracture surface exhibits characteristics typical of macroscopically brittle failure with large facets. There was no apparent corrosion, and surface appeared uniformly oxidized. In addition, there was no significant plastic deformation on the sample.

The test samples were sectioned from the failed tube support and then prepared using standard metallographic techniques. The samples were electrolytically etched with a KOH, and water solution was used to identify the carbides that were present in the microstructure. Microstructural characterization consisted of optical (OM) and scanning electron microscopes (SEM). Chemical compositions of



Fig. 1 Fracture surface of one of the furnace tube support samples-HK-40



Fig. 2 Cross section of the HK-40 sample, etched, KOH

the phases were determined without standards using an energy-dispersive spectrometer (EDS) system that was attached to the SEM. Figure 2 shows an optical micrograph of a sample showing cross section of the fracture surface in the as-etched condition showing dendritic microstructure typical of cast materials.

A SEM micrograph showing a location just below the surface of the fracture is shown in Fig. 3. The entire surface has been oxidized. In the area of the same figure, sigma- σ -phase has been identified with aid of EDS. Figure 4 shows an image of an area within the sample along with its identified phases and was again present.

Figures 5–7 show different locations within the sample. These locations also contain σ -phases and secondary carbides precipitates. Cracks were observed in the samples, and these cracks were filled with oxides. Figures 8 and 9 are optical micrographs of a sample etched using a sigma-phase etchant. It is clear that the cross section of the fracture surface exhibited an excessive amount of σ -phases along grain boundaries and along the fracture surface itself.

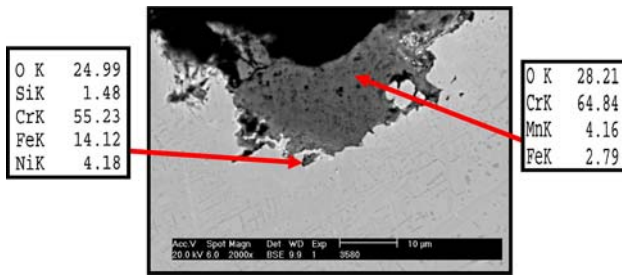


Fig. 3 SEM optical micrographs showing cross section sample in the as-polished condition along with its EDS analysis. Elemental analysis indicates oxide formation

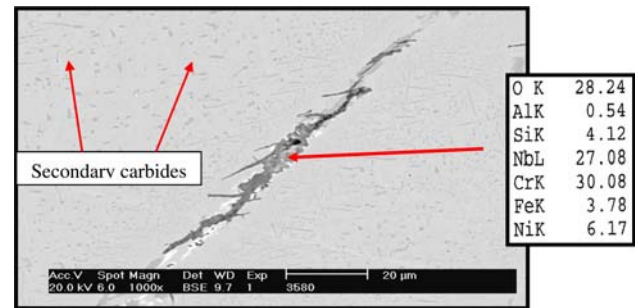


Fig. 6 Scanning electron micrograph along with its EDS analysis showing cracking filled with oxides

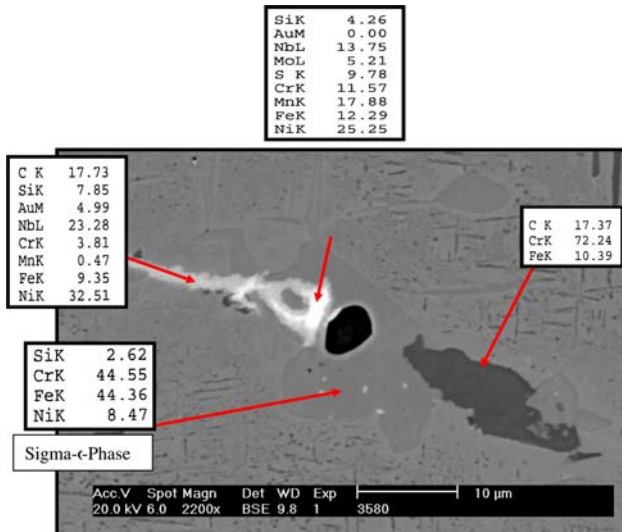


Fig. 4 Scanning electron micrograph of an inner section within a sample below the fracture surface along with EDS analysis. Composition of lower part is typical of sigma phase. High-temperature attack on σ -phase

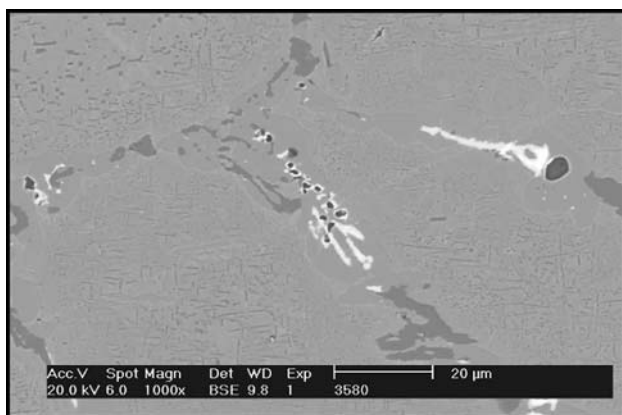


Fig. 5 Scanning electron micrograph showing signs of high-temperature attack mainly on sigma phase location

It is also clear that the areas adjacent and below σ -phases were depleted of Cr, Si, and Ni. This has prevented formation of SiO_2 and Cr_2O_3 , as clearly shown in Fig. 8 and 9

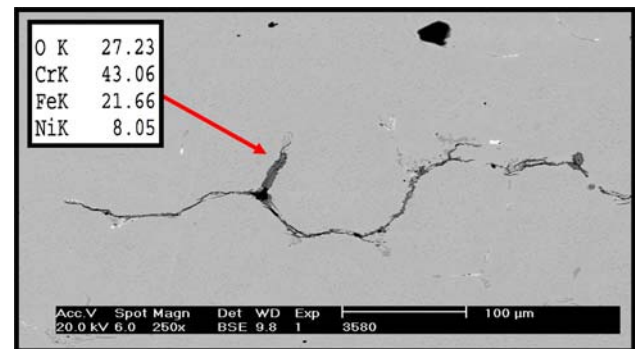


Fig. 7 Scanning electron micrograph along with its EDS analysis showing high-temperature cracking mainly following sigma phase locations

and promoted oxidation of the alloy. In addition, the stringers also have transformed into σ -phase. Cracking is interdendritic.

Materials characterization was possible with the use of an x-ray fluorescence spectrometer (XRF). Table 1 lists the results of this analysis. Major elements are within the range of that of HK40.

To understand the mechanical properties of the alloy after the in-service exposure, a tensile test was carried out. Tensile testing was carried out at room temperature and at 800 °C. The room-temperature tensile testing was done on a universal testing machine, while the tests at elevated temperature were conducted in the Gleeble machine. For the 800 °C tests, the samples were heated to 800 °C at 5 °C/s, and then kept at 800 °C for 3 min before testing. Two samples were tested at each of the temperatures (Table 2 and 3).

Results of the tensile samples are shown in Fig. 10 to 13. There is clearly only limited yield on most of the graphs (Fig. 13). The room-temperature samples broke with very little elongation. The two 800 °C samples, on the other hand, showed a little ductility, which is also reflected in the obvious reduction in area (%A).

The fact that the maximum strength values are about the same for both the room temperature and the 800 °C

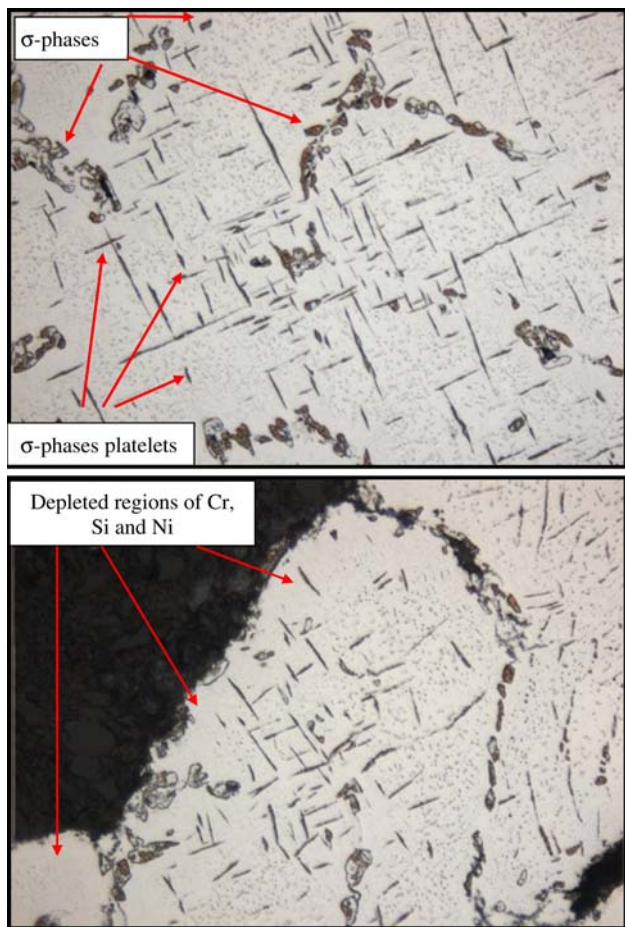


Fig. 8 Optical micrographs of the samples in the as etched condition, showing excessive amount of sigma phase. Sigma phase etchant was used

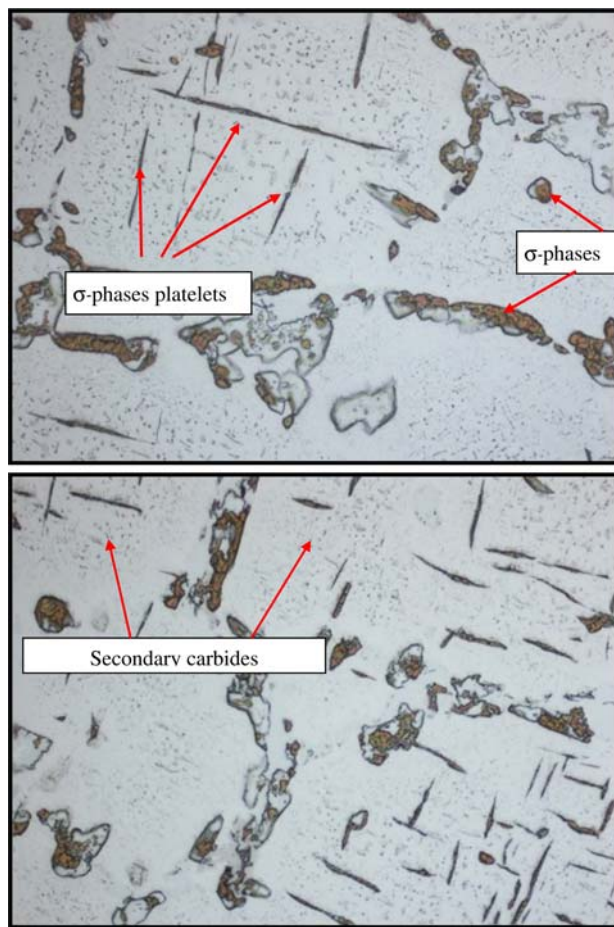


Fig. 9 Optical micrographs of the samples in the as-etched condition showing sigma phases and secondary carbides precipitates

samples is really the result of the room-temperature brittleness of the material. The room-temperature samples broke very soon after yield, while the maximum strength for the 800 °C samples is close to the ultimate tensile strength of the material at that temperature. All of the fracture surfaces showed interfacial fracture; although the samples in the 800 °C test exhibited large areas of ductile rupture.

Average hardness of two samples taken from both fracture surfaces were Rockwell B (HRB) 96.2 and 96.5 or Brinell (HB) 210 to 220. Nominal hardness of as-cast HRB 91.5 or HB 190 and as aged HB192 according to ASTM A 351/A 351 M. The difference between the various samples was not much.

Discussion

Sigma (σ) phase (iron-chromium compound) developed in the steel as shown in Fig. 4 to 9. This phase is a hard brittle

Table 1 Nominal and measured chemical compositions (wt.%) of tube materials

Element	XRF Measured	HK-40/Cast Nominal	
		Min%	Max%
C	0.39	0.35	0.45
Al	0.01		
Si	1.09	0.5	1.5
S	0.013	...	0.03
P	0.015	...	0.03
Ti	0.011		
V	0.058		
Cr	25.38	23	27
Mn	0.69	0.4	1.5
Fe	bal		
Ni	19.48	19	22
Cu	0.01		
Nb	0.195		
Mo	0.03		

Table 2 Tensile results of tree support samples tested in room and 800 °C

Sample	0.2% Proof stress, MPa	UTS, MPa	Reduction area (A), %	Elongation, %
RT1	419	495	0.7	1.0
RT2	376	470	0.8	1.0
800 °C—1	200	496	13.5	...
800 °C—2	212	478	28.9	...

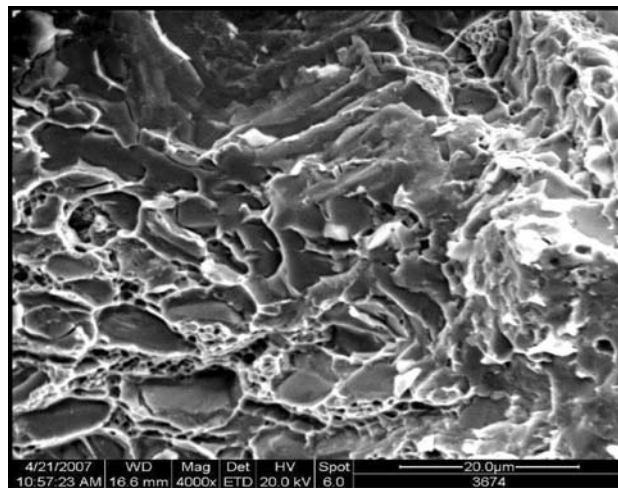
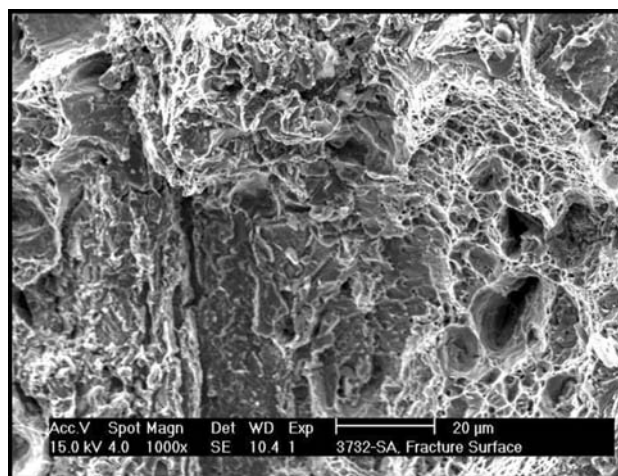
UTS, ultimate tensile strength

Table 3 Nominal mechanical properties (ASTM A 351)

Grade and UNS	Tensile Strength		Yield Strength		Elongation, %
	ksi	MPa	ksi	MPa	
HK40	62	425	30	240	10.0

**Fig. 10** Tensile samples at room temperature (RT-top) and at 800 °C after the test. The samples of the RT show no plastic deformation, indicative of brittle fracture; while slight necking is observed in the high-temperature tests

intermetallic and has a direct effect on the mechanical property of the metal. Sigma phase can form when the service temperature is within 565 to 952 °C (1050 to 1700 °F). The upper limit for sigma-phase formation varies from 870 to 980 °C (1600 to 1800 °F) [28, 35]. Sigma-phase embrittlement in 18–8 stainless steels usually occurs slowly at low temperatures, and only about 2% to 3% sigma phase will show in its macrostructure after 10 years at 650 °C (1200 °F) [36]. However, at 900 °C, sigma phase forms within a couple of minutes [37, 38].

**Fig. 11** Fracture surface of the tensile sample after testing at room temperature, showing interfacial fracture along sigma phase precipitates**Fig. 12** Fracture surface of the tensile sample after testing at 800 °C showing mixed-mode fracture and microvoids coalescence

The exposure temperature was well within the limits for sigma-phase formation, and embrittlement can readily occur. Although sigma phase was detected and its effect on the material embrittlement has been well established, it was not the sole cause of this failure. It was more of an assistant.

Sigma (σ) phase is hard and fragile, and its formation causes loss of toughness. In addition, when formed, it consumes chromium and molybdenum present within the matrix, which leads to the depletion in these elements. Sigma phase is usually not detrimental at high temperature, but promotes function when the component is cooled below 260 °C (50 °F) because of an almost complete loss of toughness [39]. The problem becomes serious when the phase is continuous, as in our case. In addition to the

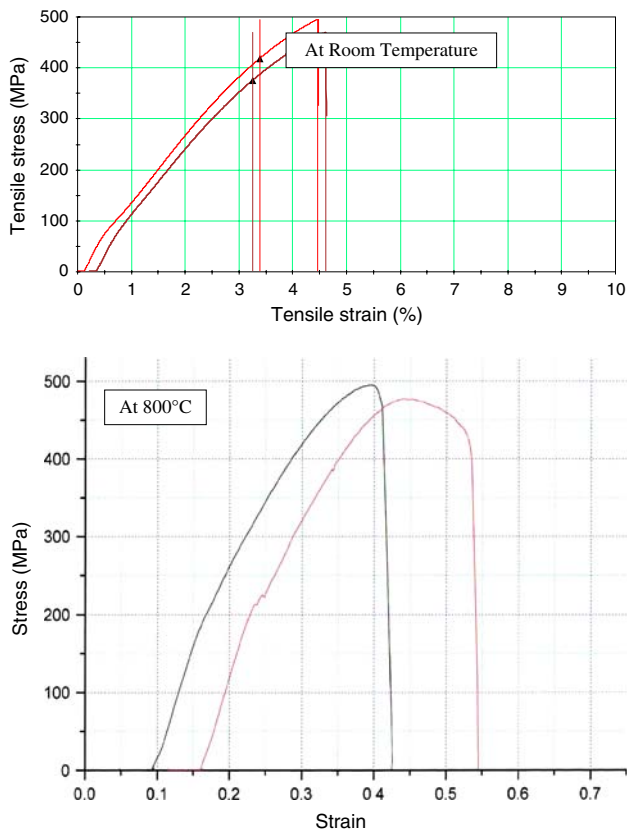


Fig. 13 Tensile tests stress and strain graphs of the samples tested at room temperature (top) and at 800 °C (bottom)

brittleness, the presence of sigma phase enhances a tendency for intergranular corrosion along the sigma precipitates.

Iron-base alloys with high chromium contents 18 to 25 wt.% are generally prone to brittle sigma-phase formation during prolonged exposures above 650 °C, and alloys with nickel contents greater than 30 wt.% are less prone to sigma formation but are more susceptible to corrosion in high-temperature environments. The precipitation of Fe-Cr sigma phase, which occurs predominantly at grain boundaries in the alloy, can also lead to considerable reduction in creep ductility at elevated temperatures in addition to the loss of fracture toughness when the components are cooled to room temperature. The strength data presented earlier are based on short-time test data and do not totally account for the property reduction due to microstructural changes in the alloy [40]. In this investigation, typical sigma-phase composition was 45% Fe, 44% Cr, 9% Ni, and 3% Si and is consistent with other investigators findings [10, 41].

As normally produced, the HK alloy type is stable austenitic over its entire temperature range of application. The as-cast microstructure consists of an austenite matrix containing massive carbides as scattered islands or networks. After aging at service temperature, the alloy exhibits a dispersion of fine, granular carbides within the

austenite grains, with subsequent agglomeration if the temperature is high enough. These fine, dispersed carbides contribute to the creep strength of the alloy. The most susceptible site for the formation of sigma phase is the grain boundaries, and the formation of this phase was possible in this cast material because of its dendritic microstructure [42].

A lamellar (stringers) constituent tentatively identified as an austenite, carbonitride eutectoid resembling pearlite also is frequently observed in HK alloys [40]. If these phases are present in excessive amounts, the unbalanced composition of the alloy can lead to the presence of some ferrite in the austenite matrix. This will directly affect the local metallurgical and mechanical properties. This ferrite, given time, will transform to the brittle sigma phase if the alloy is held around 816 °C (1500 °F) with consequent weakening at this temperature and embrittlement [43]. The direct implication of sigma-phase precipitation and growth will cause Cr and Si depletion in the surrounding metallic matrix next to it (Fig. 8) and will further reduce HK-40 metal oxidation resistance [44].

Formation of sigma phase in HK type alloy can occur directly from austenite in the range 760 to 871 °C (1400 to 1600 °F) particularly at the lower carbon level (0.20–0.30%), and for this reason a substantial breakup in properties at halfway temperatures is observed for this grade [45]. Comparing other alloys, for instance, other alloys with higher nickel, in the same environment would be beneficial. The higher the nickel, the more stable the austenitic structure, which imparts high-temperature corrosion resistance. In addition, nitrogen stabilizes austenite, which results in the control of sigma formation [46] and at time resistance [47–49]. However, in the failed furnace tube support, the formation of sigma phase resulted in the degradation of material properties and in unsuitable performance.

Conclusions

In this study, microstructural and mechanical properties changes in HK-40 subjected to sigma-phase formation were characterized and determined to degrade the performance of the furnace tube support. Sigma-phase precipitation and growth advances, at 850 °C, caused Cr and Si depletion in the surrounding matrix and resulted in a reduction in HK-40 performance.

References

1. Failure Analysis and Prevention, vol. 11. ASM Handbook, ASM International, Materials Park, OH (1996)
2. Colangelo, V.J., Heiser, F.A.: Analysis of Metallurgical Failures, 2nd edn., Wiley, New York (1987)

3. El-Batahgy, A., Zaghoul, B.: Creep failure of cracking heater at a petrochemical plant. *Mater. Charact.* **54**(3), 239–245 (2005)
4. Kumar, R.A., Sinha, S.K., Tiwari, Y.N., Swaminathan, J., Das, G., Chaudhuri S.: Analysis of failed reformer tubes. *Eng. Fail. Anal.* **10**, 351–358 (2003)
5. Ashby, M.F.: Deformation-mechanism, maps. *Acta Metall.* **20**, 887–897 (1972)
6. Dyson, B.: Use of CDM in materials modeling and component creep life prediction. *J. Pressure Vessel Technol.* **122**, 281–296 (2000)
7. Ejaz, N., Tauqir, A.: Failure due to structural degradation in turbine blades. *Eng. Fail. Anal.* **13**(3), 452–463 (2006)
8. Barbosa, C., Nascimento, J.L., Caminha, I.M.V., Abud, I.C.: Microstructural aspects of the failure analysis of nickel base superalloys components. *Eng. Fail. Anal.* **12**(3), 348–361 (2005)
9. Pang, H.T., Reed, P.A.S.K.: Microstructure effects on high temperature fatigue crack initiation and short crack growth in turbine disc nickel-base superalloy Udimet 720Li. *Mater. Sci. Eng. A* **448**(1–2), 67–79 (2007)
10. Coreño-Alonso, O., Duffus-Scott, A., Zánchez-Cornejo, C., Coreño-Alonso, J., de Jesús, F.S., Bolarín-Miró, A.: On the effect of σ -phase formation during metal dusting. *Mater. Chem. Phys.* **84**(1), 20–28 (2004)
11. Kobayashi, K., Yamaguchi, K., Hayakawa, M., Kimura, M.: Grain size effect on high-temperature fatigue properties of alloy 718. *Mater. Lett.* **59**(2–3), 383–386 (2005)
12. Bulloch, J.H., Bernard, P.J.: A remaining life assessment of a cracked attemporator steam line. *Eng. Fail. Anal.* **8**(6), 529–540 (2001)
13. Shang, D.G., Sun, G.Q., Yan, C.L., Chen, J.H., Cai, N.: Creep-fatigue life prediction under fully-reversed multiaxial loading at high temperatures. *Int. J. Fat.* **29**(4), 705–712 (2007)
14. Inoue, T., Okazaki, M., Igari, T., Sakane, M., Kishi, S.: Evaluation of fatigue-creep life prediction methods in multiaxial stress state. *Nucl. Eng. Des.* **126**, 13–21 (1991)
15. Ogata, T., Yaguchi, M.: Damage mechanism in weldment of 2.25Cr–1Mo steel under creep-fatigue loading. *Eng. Fract. Mech.* **74**(6), 947–955 (2007)
16. Elmer, J.W., Palmer, T.A., Specht, E.D.: In situ observations of sigma phase dissolution in 2205 duplex stainless steel using synchrotron X-ray diffraction. *Mater. Sci. Eng. A* **459**, 151–155 (2007)
17. Kington, A.V., Noble, F.W.: σ phase embrittlement of a type 310 stainless steel. *Mater. Sci. Eng. A* **138**(2), 259–266 (1991)
18. Barcik, J.: The kinetics of σ -phase precipitation in AISI310 and AISI316 steels. *Metall. Mater. Trans. A* **14**(3), 635–641 (1983)
19. Solomon, H.D., Devine, T.M.: In: Lula, R.D. (ed.) *Duplex Stainless Steels*, pp. 693–756. American Society for Metals, Metals Park, OH (1983).
20. Sedriks, J.: *Corrosion of Stainless Steels*, 2nd edn., p. 22. John Wiley & Sons, New York (1996)
21. Jahromi, S.A.J., Javadpour, S., Gheisari, Kh.: Failure analysis of welded joints in a power plant exhaust flue. *Eng. Fail. Anal.* **13**(4), 527–536 (2006)
22. Honeycombe, R.W.K.: *Steels: Microstructure and Properties*, 2nd edn. Arnold, London (1995)
23. Brett, S.J.: In-service cracking mechanism affecting 2CrMo welds in 1/2CrMoV steam pipework systems, Proc. International Conference on Integrity of High-Temperature Welds, IOM, pp. 3–14 (1998).
24. Peckner, D., Bernstein, I.M.: *Handbook of Stainless Steels*. McGraw-Hill (1977).
25. Lamb, S., Bringas, J.E. eds.: *Practical Handbook of Stainless Steels and Nickel Alloys*. ASM International, Materials Park, OH (1999)
26. Blair, M.C.: *Cast Stainless Steels*, Metals Handbook, vol. 1, p. 908. ASM International, Materials Park, OH (1990)
27. Zhu, S.J., Wang, Y., Wang, F.G.: Comparison of the creep crack growth resistance of HK40 and HP40 heat-resistant steels. *J. Mater. Sci. Lett.* **9**(5), 520–521 (1990)
28. Pankiw, R.I., Voke, D.P., Muralidharan, G., Evans, N.D., Stevens, C.O., Liu, K.C., Santella, M.L., Maziasz, P.J., and Sikka, V.K.: Precipitation and its effect on the design of cast heat resistant alloys, *Corrosion/2007*, paper 7424
29. Authors' personal investigative experiences
30. Ezuber, H.M., El-Houd, A., El-Shawesh, F.: Effects of sigma phase precipitation on seawater pitting of duplex stainless steel. *Desalination* **207**, 268–275 (2007)
31. Lope, N., Cid, N., Puiggali, M.: Influence of σ -phase on mechanical properties and corrosion resistance of duplex stainless steels. *Corrosion Science* **41**(8), 1615–1631 (1999).
32. Johnson, E., Kim, Y.J., Chumbley, L.S., Gleeson, B.: Initial phase transformation diagram determination for the CD3MN cast duplex stainless steel. *Scr. Mater.* **50**(10), 1351–1354 (2004)
33. Wilms, M.E., Gadgil, V.J., Krougman, J.M., Kolster, B.H.: Effect of σ -phase precipitation at 800 °C on the mechanical properties of a high alloyed duplex stainless steel. *Mater. High Temp.* **9**(3), 160–166 (1991)
34. Patankar, S.N., Tan, M.J.: Sigma phase precipitation during superplastic forming of duplex stainless steel. *Mater. High Temp.* **19**(1), 41–44 (2002)
35. Blair, M.C.: *Cast Stainless Steels*, Metals Handbook, vol. 1, p. 908. ASM International, Materials Park, OH (1990)
36. Hansen, D.A., Puyear, R.B.: *Materials Selection for Hydrocarbon and Chemical Plants*. Marcel Dekker (1996)
37. Hau, J., Seijas, A.: Sigma phase embrittlement of stainless steel in FCC service, *Corrosion/2006*, paper 06578
38. *Corrosion*, vol. 13, p. 11. Metals Handbook, ASM International, Metals Park, OH (1987)
39. Li, J., Wu, T., Riquier, Y.: Sigma phase precipitation and its effect on the mechanical properties of a super duplex stainless steel. *Mater. Sci. Eng. A* **174**, 149–156 (1994)
40. Tiong, D.K-K, Walsh, J., McHaney, J.H.: Technical challenges in using super duplex stainless steel. *Corrosion/2006*, paper 6147
41. Vander Voort, G.F.: *Properties and Selection: Iron Steels and High-Performance Alloys*, vol. 1, 10th edn., p. 709. Metals Handbook, ASM International, Materials Park, OH (2001)
42. Kobayashi, D.Y., Wolyne, S.: Evaluation of the low corrosion resistant phase formed during the sigma phase precipitation in duplex-stainless steels. *Mater. Res.* **2**(4), 239–247 (1999)
43. Natesan, K.: Materials performance in coal fluidized bed combustion environment. Tenth International Pittsburgh Coal Conference, Pittsburgh, PA, 20–24 Sept 1993
44. Sedriks, A.J.: *Corrosion of Stainless Steels*, 2nd edn. John Wiley & Sons (1996)
45. Zucato, I., Moreira, M.C., Machado, I.F., Lebrao, S.M.: Microstructural characterization and the effect of phase transformations on toughness of the UNS S31803 duplex stainless steel aged treated at 850 °C. *Mater. Res.* **5**(3), 385–389 (2002)
46. *Steel Castings Handbook Supplement 9 High Alloy Data Sheets Heat Series Steel Founders' Society of America* (2004)
47. Dove, D., Messer, B., Phillips, T.: An austenitic stainless steel, resistant to high temperature creep and naphthenic acids attack in refinery environments. *Corrosion/2001*, paper 01523
48. Nicolio, C.J., Holmquist, M.: Duplex alloys; challenging corrosion in the new millennium. *Corrosion/2002*, paper 02120
49. Tang, Y.J., Wang, Q.M., Yuan, F.H., Gong, J., Sun, C.: High-temperature oxidation behavior of arc ion plated NiCoCrAlYSiB coatings on cobalt-based super alloy. *J. Mater. Res.* **21**(3), 737 (2006)